EFFECT OF HOLD TIME ON ELEVATED-TEMPERATURE LOW-CYCLE FATIGUE

N. OHTSUKA

Civil & Applied Mechanics Research Team, Kawasaki Laboratory,
Chiyoda Chemical Engineering & Construction Co., Ltd., Kawasaki-ku, Kawasaki 210, Japan

SUMMARY

The periodic time in low-cycle fatigue tests at elevated-temperature is extremely shorter, in general, than in practical structures and has an important effect on the fatigue life.

In order to investigate the effect of time, isothermal fatigue tests were conducted on Type SUS32PH (equivalent to AISI 316) stainless steel at room temperature, 550°C, and 800°C, and on 1 Cr-1/4 Mo steel, SCM3, at the temperature of 550°C, using an electro-hydraulic servo-control universal thermal fatigue testing machine developed by the authors. The specimens were maintained the desired strain range throughout the test and kept the strain constant during the tensile and compressive hold times ranging from 0.3 to 995 seconds.

A considerable reduction in fatigue life was observed when the test temperature was raised and the hold time period was increased.

The linear fraction rule between creep and fatigue damage was compared with the experimental results, and it was found that there lie several problem points of significance in the rule, especially in relation to cyclic softening materials such as SCM3 steel. Therefore, we considered that the creep effect did not so seriously dominate over the straincontrolled fatigue life at elevated-temperature and discussed further as follows.

In case of corrosion fatigue, Endo *et al.* assumed that reduction of fatigue strength with decreasing the cycle frequency was due to the notch effect of corrosion pits, and indicated that various experimental results were well explained by applying the corrosion effect or notch effect, K, which is the ratio of the fatigue strength in air to the one under corrosion at the same number of cycles.

Modifying this criterion to low-cycle fatigue at elevated temperature, the following life evaluating equation formulating the relationships among the cyclic dependency effect by fatigue damage, the time dependency effect by oxidation, and the combined effect, was developed from a study of the experimental results in this paper:

$$(1+B.t_o^{n_1}.N_f^{n_2}).\varepsilon_{pR}.N_f^{\alpha_0} = C_0$$

where, t_0, ε_{pR}, and N_f are the hold time during a half cycle, plastic strain range, and the number of cycles to failure, respectively, and B, n_1, n_2, α_0, and C_0 are constants. The time dependency effect may be interpreted also to include other supplementary effects such as creep damage and deterioration of materials.

1. Introduction

With the progress of the reactor technology in recent years, reactor components are increasingly used in a temperature range exceeding the creep limit. In such a temperature range, the relations between stress and strain of metallic materials change with time, and moreover their fatigue lives are influenced by time. The range of periods of loading cycles in actual component is vast, and the difference from the period range of cycles of fatigue tests conducted in laboratories is also great. For this reason, it has becomo a vital problem to evaluate the effect of the time.

In our study described in this paper, for clarifying the effect of the time in the elevated-temperature low-cycle fatigue, strain-controlled fatigue tests were conducted on two types of steel materials by changing the hold time of the trapezoidal strain waveform at a constant temperature in the creep range.

2. Experiments

The materials tested were austenite stainless steel SUS32HP (equivalent to AISI 316) which was solution heat treated and quenched and tempered 1Cr-1/4 Mo steel SCM3. The chemical compositions of the materials are shown in Table 1 and their mechanical properties in Table 2. Two types of test specimens in the shape of thin hollow cylinders of 10 mm in inner diameter and 12.4 mm in outer diameter as shown in Fig. 1 were used.

By means of an electrohydraulically servo-valve controlled universal thermal fatigue testing machine developed by the authors, strain-controlled fatigue tests were conducted by repeatedly giving a trapezoidal wave strain shown in Fig. 2 in the axial direction at a constant temperature. The conditions of the experiment are shown in Table 3.

The specimens were heated by passing an electric current through them. The temperature of the specimen was detected by means of two couples of chromel-alumel thermocouples spot-welded on the center of the test specimen, one of which was used for the automatic control feedback circuit to keep the temperature of the specimen at a constant level during the test. The load applied to the specimen was detected by a load cell.

For the fatigue test of SUS32 steel, interchuck displacement control was conducted by means of DTF (differential transformer). And the strain was microscopically detected after reading the shift of the marking lines with an interval of 10 mm marked on the parallel part of the test specimen. This strain was kept constant during the experiment through successive adjustment. In the case of SCM3 steel, in order to increase the detection accuracy of the strain to be controlled and to realize perfect automatization of the experiment, a DTF was mounted on the collars having an interval of 25 mm at the center of the test specimen for detection and control of the displacement. Moreover, the strain for an interval of 10 mm in the center of the test specimen was measured microscopically to obtain a calibration curve, which was used for converting the displacement between the collars into correct strain values.

3. Experimental Results

3.1 Variation of Stress

When trapezoidal strain waveforms were repeatedly applied to the test specimen at temperatures in the creep range, stress relaxation was caused during the hold time of the peak strain. The representative hysteresis loop in the experiment was as shown in Fig. 3, and the values in the figure have the following relationships:

$$\varepsilon_{pR} = \varepsilon_{tR} - \varepsilon_{eR} \quad (1)$$

$$\varepsilon_{eR} = \sigma_{1R}/E \quad (2)$$

$$\varepsilon_{c} = \sigma_{c}/E = (\sigma_{uR} - \sigma_{1R})/(2E) \quad (3)$$

where ε_{pR}, ε_{eR}, ε_{tR} are the plastic strain range, elastic strain range and total strain range, respectively, while ε_{c} shows the creep strain corresponding to the stress relaxation. And σ_{uR} and σ_{1R} are respectively the upper stress range (the stress immediately after loading) and the lower stress range (the stress immediately before unloading), while E is the modulus of longitudinal elasticity of the material at the test temperature.

In the strain-controlled fatigue tests, the stress range applied to the test specimen showed different variations during the life depeding upon the type of the material and the test conditions. In the case of SUS32 steel, as shown in Fig. 4, there was a tedency to increase the stress range with the repeated strains and to cause cyclic strain hardening till cracks were caused in the test specimens, although the degree varied depending upon the test conditions. Conversely, in the case of SCM3 steel at 550° C, as shown in Fig. 5, a cyclic strain softening tendency was obserbed, although varying in degree depending upon the test conditions.

In this manner, the stress range applied to the test specimen varied during the test, so that the value at about half of the number of cycles to failure N_f was used as the stress range of the test specimen. The relationship between this individual stress range and the strain range of each test specimen (dynamic stress-strain relationship), as shown in Fig. 6 and Fig. 7, was influenced by the cyclic strain hardening tedency or the cyclic strain softening tendency as well as the stress relaxation due to creep of the material. Particularly in the case of SCM3 steel which showed a marked tendency of the cyclic strain softening, the lower stress range varied complicatedly depending upon the strain range, as shown in Fig. 7.

3.2 Fatigue Life Curve

In this experiment, the fatigue life (the number of cycles to failure) N_f of the specimen was defined as the period when macro cracks due to fatigue reached a half to one third of the total periphery of the specimen. The relationships between the plastic strain range ε_{pR} applied to the specimens of SUS32 steel and SCM3 steel and the number of cycles to failure N_f are as shown in Fig. 8 and Fig. 9. A nearly linear relationship was obtained for each test condition, in which the following Manson-Coffin formula ([1] , [2]) applies:

$$\varepsilon_{pR} \cdot N_f^{\alpha} = C \quad (4)$$

Where α and C are constants.

When the results of the tests under various test temperature conditions in the case of 2 x 5 sec. in the strain holding time for SUS32 steel in Fig. 8 are compared, the number of cycles to failure decreases with the increase in the test temperature. A decrease in the fatigue life due to the increase in the hold time is not observable at 550°C, but is markedly seen at 800° C, and its fatigue curve has a sharper gradient, showing the effect of the time (hold time at peak strain) upon the fatigue life. The results of the test for SCM3 steel at 550°C shown in Fig. 9 indicate the effect of the strain holding time, similar to the case of

SUS32 steel at 800°C.

4. Discussion

4.1 Effect of Hold Time on Elevated-Temperature Low-cycle Fatigue

As described in experimental results, the effect of hold time upon the elevated-temperature low-cycle fatigue appeared in the range of this experiment on SUS32 steel at 800° C and that of SCM3 steel at 550° C. If we show the plastic strain range ε_{pR} as the parameter for these two cases to see the decrease in the number of cycles to failure N_f due to the increase in the hold time $2t_o$ in one cycle from Fig. 8 and Fig. 9, it will be as shown in Fig. 10. According to this figure, the rate of decrease in the fatigue life N_f due to the increase in the hold time $2t_o$ rises with the decrease in the strain range, and in the case of SUS32 steel at 800° C, it becomes more conspicuous with the increase in the hold time as Krempl and Walker [3] have shown.

The relationship between the elevated-temperature fatigue life defined as the total time to failure t_f and the total strain range ε_{tR} for SUS32 steel and that for SCM3 steel are respectively shown in Fig. 11 and Fig. 12. If we compare these figures with Fig. 8 and Fig. 9 showing the relationships with the number of cycles to failure N_f, we find that, under the same temperature condition, the life t_f increases with the increase in the hold time, conversely to the case of N_f. Morecover, with the increase in the strain range, the ε_{pR}-N_f curves of the various hold times draw nearer to become cycle dependent, but with the decrease in the strain range, the ε_{tR} - t_f curves draw nearer to become time dependent.

The relationships between the cyclic stress σ applied to the specimens at 1/2 N_f and the total time to failure t_f regarding two types of materials are shown in Fig. 13 and Fig. 14. For references, the static creep rupture curves at 550°C and 800°C interpolated between the curves from the literature [4] are shown in Fig. 13, and the static creep rupture data with the identical shaped specimens with the fatigue specimens in Fig. 1(b) are also included in Fig. 14.

4.2 Linear Life Fraction Rule for Fatigue and Creep

A linear or cumulative damage rule which maintains that the principal cause of the decrease in the elevated-temperature low-cycle fatigue life due to an increase in the strain holding time described in the preceding paragraph is attributable to accumulation of creep damage and fatigue damage caused during the load cycles has been used by many investigators. Here fatigue damage ϕ_f and creep damage ϕ_c are generally given by the following equations (Campbell 5) :

$$\phi_f = \sum_{o}^{p} (N_f/N_{fo}) \qquad (5)$$

$$\phi_c = \sum_{o}^{H} (t_h/t_r) \qquad (6)$$

where

N_f = the number of cycles to failure of a given strain range ε_R

N_{fo} = the number of cycles to failure at strain range ε_R for the range of strain rates applicable.

t_h = the incremental time at a stress level σ

t_r = the time-to-rupture at stress σ.

There are several rules proposed for experessing the relationship between ϕ_f and ϕ_c (Wood [6] , Manson and Halford [7]), but the simplest and most popular is the

following (Manson et al. [8], Campbell [5]).

$$\phi_f + \phi_c = D \qquad (7)$$

where D = total damage factor.

In the case of a strain-controlled fatigue test at a temperature in the creep range, stress relaxation is caused during the hold time at the peak strain and the value of the stress is varied, so that it is necessary to use the following Eq. (8) instead of Eq. (6) as the creep damage ϕ_c and to integrate over the strain holding time.

$$\phi_c = 2N_f \cdot \int_o^{t_o} dt/t_r \qquad (8)$$

The stress σ at t hours after reaching the upper stress σ_u can be expressed by the following equation as shown in Fig. 15:

$$\sigma = \sigma_o (t + \triangle t)^{-\gamma} \qquad (9)$$

where σ_o, $\triangle t$, and γ are constants.

From this, constant γ is calculated as follows:

$$\gamma = \log (\sigma_u / \sigma_\ell) / \log (1 + t_o / \triangle t) \qquad (10)$$

where t_o is the strain holding time in half a cycle and σ_ℓ, the lower stress. On the other hand, the time-to-rupture t_r at stress σ is experessed, in general, as follows:

$$\sigma = C_* \cdot t_r^{-n} \qquad (11)$$

where C_* and n are constants.

Therefore, substituting Eq. (9) and Eq. (11) into Eq. (8), and taking D=1 in Eq. (7), we can calculate the estimated value of the fatigue life by the following equations:

$n \neq \gamma$:

$$\frac{1}{N_f} = \frac{1}{N_{fo}} + \frac{2 \cdot \sigma_\ell^{1/\gamma} \cdot (t_o + \triangle t)}{\gamma \cdot C_*^{1/n} \cdot (1/n - 1/\gamma)} (\sigma_u^{1/n-1/\gamma} - \sigma_\ell^{1/n-1/\gamma}) \qquad (12)$$

$n = \gamma$:

$$\frac{1}{N_f} = \frac{1}{N_{fo}} + \frac{2 \cdot \sigma_u^{1/n} \cdot \triangle t}{n \cdot C_*^{1/n}} \ell n (\frac{\sigma_u}{\sigma_\ell}) \qquad (13)$$

Regarding SUS32 steel at 800°C and SCM3 steel at 550°C, the fatigue lives sought by means of Eq. (12) or Eq. (13) using constants in Eq. (11) obtained from the conventional creep rupure curves in Fig. 13 and Fig. 14 are compared with the experimental results in Fig. 16 and Fig. 17. For SUS32 steel at 800°C as shown in the figure, the estimated value with the hold time of 2 x 95 sec. is conservative, while the estimated value with 2 x 995 sec. is on the dangerous side and the difference from the experimental value is large. In the case of SCM3 steel at 550°C, as shown in Fig. 17, the estimated values are considerably different from the experimental points, and no clear regularity is obtained. The results are plotted in Fig. 18 to show the correlation between the fatigue damage ϕ_f and the creep damage ϕ_c. The solid line in the figure indicates Eq. (7) when D = 1 (Manson et al. [8]), the broken line indicates the case of D obtained by statistical treatment of the experimental results (Campbell [5]). According to the figure, these two types of D do not agree with the experimental results, and moreover, values on the dangerous side are sometimes given, showing little clear correlation between the fatigue damage ϕ_f and the creep damage ϕ_c.

In case of the stress-controlled fatigue test, the stress is kept constant during the

load holding time as shown in Fig. 19(I) and the stress level is not affected by the deformation, so that it appears that linear fraction rule to correlate with the static creep strength is applicable mostly (Robinson [9], Taira [10]). On the other hand, in case of the strain-controlled fatigue test, the stress level decreases to a low level due to stress relaxation during the strain holding time as shown in Fig. 19 (II), and more the creep deformation is yielded, more the stress level is lowered. Therefore there arises a question whether it is reasonable to consider that the creep damage in Eq. (7) is large enough as compared with the other damages to be discussed in the following paragraph, and that creep damage is accumulated during such a strain-controlled test.

Although the linear damage rule by Eq. (7) is relatively easily applicable to practical design, it is considered that it involves the following problem points in view of this experimental results.

(1) In the strain-controlled elevated-temperature fatigue unlike the case of a stress-controlled fatigue, the estimated value of life by Eq. (7) does not agree well with the experimental results, and moreover, as shown in Fig. 18, values on the dangerous side are obtained sometimes, which should be noted.

(2) In general, the creep rupture curve of a material has a small gradient, so that a slight variation in the stress applied to the test specimen tends to vary the fatigue life N_f calculated from Eq. (7) more greatly than the experimental result. Particularly in such a cyclic strain softening material as SCM3 steel, the lower stress range in the dynamic stress-strain relationship shown in Fig. 7 varies in a complicated manner, making it difficult to apply Eq. (7). Moreover, for evaluating Eq. (7), it is necessary to know the details of the stress history during the strain cycling test, which is difficult to attain in general.

(3) Although the denominator t_r in Eq. (8) was obtained from the conventional creep rupture curve in this sudy, there is also the problem of whether the stress under stress relaxation caused during the holding time in a strain-controlled test and the stress varying with the load cycles can be treated similarly to the stress in the case of static creep and of how to evaluate the influence of strain history. Static creep tests by means of notched specimens (Spera [11]) and dynamic creep tests by means of smooth test specimens (Manson et al. [8]) have been conducted to obtain a proper curve for the creep rupture curve as Eq. (11), but the execution of such proposed methods would require considerable time and labor.

(4) In Eq. (7), the environmental effect which is assumed to have a serious effect upon the elevated-temperature fatigue life is not taken into consideration.

4.3 Environmental Effect on Elevated-Temperature Low-Cycle Fatigue

White et al. [12] have confirmed that the fatigue life N_f increases when an elevated-temperature fatigue test is conducted in a vacuum. Also in the present study on SCM3 steel in argon where only insufficient substitution was made, the fatigue life increased somewhat from that tested in air, as shown in Fig. 9. Coffin [13] showed that the elevated-temperature low-cycle fatigue life N_f for various frequencies conducted in vacuum or in argon is roughly in agreement with the results of a fatigue test in air at room temperature, and concluded that the environment is a more important consideration than the creep rupture properties in high temperature fatigue.

On the other hand, Endo et al. [14] considered that the decrease in the fatigue strength

in corrosion fatigue is due to the notch effect of the defect caused by the corrosion on the surface, and indicated that the corrosion fatigue can be rationally described by defining the corrosion effect or notch effect due to corrosion pits (denoted by K). Now we shall attempt to expand this theory to the elevated-temperature low-cycle fatigue region, and attributing its time-dependent effect to the corrosion effect Kp due to corrosion pits, we define Kp as follows:

$$K_p = \frac{\text{(Plastic strain range } \varepsilon_{pRO} \text{ when fatigue life without time-dependent effect is } N_f}{\text{(Plastic strain range } \varepsilon_{pR} \text{ when fatigue life with hold time is } N_f)} \quad (14)$$

Taking into consideration the simple expression of the thickness variation of oxydation corrosion film in time , the relationship between the corrosion effect Kp and the elapsed time t_o at elevated-temperature is assumed to be expressed by the following equation:

$$K_p = 1 + A \cdot t_o^{n1} \quad (15)$$

where A and n_1 are constants.

For example, in case of SCM3 steel at 550°C, the first approximate values of Kp are obtained on the assumption that the numerators in Eq. (14) are the same as ε_{pR} with the hold time of 2 x 0.3 sec. so that the (Kp-1) values are shown in Fig. 20 as solid lines. Then the ε_{pRO} without time-dependent effect are calculated on substituting Kp values for the hold time of 2 x 0.3 sec. found on broken lines in Fig. 20 into Eq. (14), and the second approximate values of Kp are given by Eq. (14) on the basis of the ε_{pRO}. After repeating this process several times, the satulated values of Kp are obtained to prove Eq. (15) as in Fig. 21. Similarly, with regard to SUS32 steel at 800°C, Eq. (15) is satisfied, as shown in Fig. 22.

Constant A of Eq. (15) is easily obtained as (Kp-1) at t_o = 1 sec. in Fig. 21 and Fig. 22, and proves to be a function of the fatigue life N_f. The relationship between the fatigue life N_f and Constant A, as shown in Fig. 23, can approximately be represented by the following equation:

$$A = B \cdot N_f^{n2} \quad (16)$$

where B and n_2 are constants.

Substituting Eq. (16) into Eq. (15), the corrosion effect Kp is represented as a function of t_o and N_f by Eq. (17), and the constants in the equation can be evaluated as follows.

$$K_p = 1 + B \cdot t_o^{n1} \cdot N_f^{n2} \quad (17)$$

In the case of SCM3 steel at 550°C: $n_1 = 0.35$, $n_2 = 0.76$, $B = 2.3 \times 10^{-3}$

In the case of SUS32 steel at 800°C: $n_1 = 0.78$, $n_2 = 0.45$, $B = 0.67 \times 10^{-3}$

If we substitute the plastic strain range ε_{pRo} obtained by substituting Eq. (17) into Eq. (14), into Eq. (4), we get

$$(1 + B \cdot t_o^{n1} \cdot N_f^{n2}) \cdot \varepsilon_{pR} \cdot N_f^{\alpha_o} = C_o \quad (18)$$

where α_o and C_o are constants in Eq. (4) when there is no strain holding time. If we put Eq. (18) as

$$C_1 + C_2 = C_o \quad \text{or} \quad C_1/C_o + C_2/C_o = 1 \quad (19)$$

$$C_1 = \varepsilon_{pR} \cdot N_f^{\alpha o} \quad (20)$$

$$C_2 = (B \cdot t_o^{n1} \cdot N_f^{n2}) \cdot \varepsilon_{pR} \cdot N_f^{\alpha o} \qquad (21)$$

and consider that the values of C in Eq. (19) to Eq. (21) are corresponded to damages, we can interpret that Eq. (18) means that a failure is caused when the sum of damage C_1 due to the fatigue and the other damage C_2 reaches the certain level of damage Co. We can rewrite Eq. (21) as

$$C_2 = B \cdot t_o^{n1} \cdot (N_f^{n2+\alpha o} \cdot \varepsilon_{pR}) = B \cdot t_o^{n1} \cdot (N_f^{\alpha 1} \cdot \varepsilon_{pR}) \qquad (22)$$

$$= B \cdot (t_o \cdot N_f)^{n1} \cdot (N_f^{n2-n1+\alpha o} \cdot \varepsilon_{pR}) = B \cdot t_f^{n1} \cdot (N_f^{\alpha 2} \cdot \varepsilon_{pR}) \qquad (23)$$

where

$$t_f = t_o \cdot N_f \,, \quad \alpha_1 = n_2 + \alpha_o \,, \quad \alpha_2 = n_2 - n_1 + \alpha_o$$

Thus C_2 is considered to be consisted of the time effect such as oxidation corrosion represented by t_o^{n1} or t_f^{n1}, and the combined effect (such as acceleration of the oxidation corrosion) with the strain cycling represented by the term including N_f. Comparing the indices n_2 for two materials in Eq. (17), it is found that SCM3 steel has a larger combined effect than SUS32 steel, which is in agreement with the observed fact that oxidation film fell off markedly from the surface of the SCM3 steel specimen during the elevated-temeprature fatigue test.

Taking C_1/C_o along the axis of abscissa and C_2/C_o along the axis of ordinates, all the experimental results regarding SUS32 steel at 800° C and SCM3 steel at 550° C are plotted in Fig. 24, approaching the solid line showing Eq. (19). Indicating the scatter band, taken as ± 0.3, of the right side of Eq. (19) in broken line in the figure, almost all the experimental points come within the broken line, showing a relatively good correlation between C_1 and C_2.

In the foregoing discussion, we have treated Kp principally as the effect due to oxidation corrosion, but actually there should be also the effects such as damage due to creep, the deterioration of the material due to precipitation and so on. Nonetheless, these various factors may be treated as being included in the term of time of Eq. (18). The values of the various constants in Eq. (18), however, should be confirmed by performing fatigue tests in vacuum and under various conditions of a wider range.

5. Conclusions

Elevated-temperature low-cycle fatigue tests in which trapezoidal strain waveforms were repeatedly given to specimens of SUS32 steel and SCM3 steel were conducted, and the effect of the strain holding time were investigated. The principal results obtained are as follows:

(1) With a rise in the temperature of the fatigue test, and with an increase in the strain holding time, the number of cycles to failure decreases markedly, and this tendency further increases when the strain applied to the test specimen is small.

(2) In the elevated-temperature fatigue, the fatigue damage due to the cyclic plastic strain is predominant in the higher strain ranges, but in the lower strain ranges, the time dependent damage becomes predominant.

(3) The linear damage rule which means that failure is caused when the sum of fatigue damage and creep damage reaches a certain level is not in good agreement with the results of this strain-controlled fatigue test, and it was found there lie several serious problems in this rule.

(4) Endo's theory regarding corrosion fatigue was modified to develop the life-evaluating equation, which takes into account the cyclic effect due to fatigue damage, the time effect due to oxidation corrosion, and their combined effect, and proved to be in considerable agreement with the experimenta results. This time effect may include other supplementary effects such as creep damage and deterioration of materials.

(5) The elevated-temperature low-cycle fatigue of materials should be treated by distinguishing the stress-controlled type which causes creep strain from the strain-controlled type which causes stress relaxation. The predominant damage of the material appears to differ between the two.

6. Acknowledgement

This work was performed under the guidance of Prof. T. Udoguchi of University of Tokyo, and the author gratefully acknwledges helpfull discussions with him.

REFERENCES

(1) MANSON, S.S., NACA TN 2933 (1953), NACA TR 1170 (1954).

(2) COFFIN, L.F., "A study of the effects of cyclic thermal stresses on a ductile metal ", Trans. ASME, 76-6 (1954), 931.

(3) KREMPL, E., WALKER, C.D., "Effect of creep-rupture ductility and hold time on the 1000°F strain-fatigue behavior of a 1Cr-1Mo-0.25V steel", ASTM STP. 459 (1968), 75.

(4) SIMMONS, W.F., CROSS, H.C., "The elevated-temperature properties of stainless steels", ASTM STP. No.124 (1952), 5.

(5) CAMPBELL, R.D., "Creep/fatigue interaction correlation for 304 stainless steel subjected to strain-controlled cycling with hold times at peak strain", Trans. ASME, J. Eng. Ind., (1971), 887.

(6) WOOD, D.S., "The effect of creep on the high strain fatigue behavior of a pressure vessel steel", Welding Research Supplement, (1966), 91.

(7) MANSON, S.S., "A simple procedure for estimating high-temperature low-cycle fatigue", Experimental Mechanics, (1968), 349.

(8) MANSON, S.S., HALFORD, G.R., SPERA, D.A., "The role of creep in high-temperature low-cycle fatigue", A.E. Johnson Memorial Volume, (1969).

(9) ROBINSON, E.L., "Effect of temperature variation on the long-time rupture strength of steels", Trans. ASME, 74 (1952), 777.

(10) TAIRA, S., "Lifetime of structures subjected to varying load and temperature", Creep in structures, N.J. Hoff, ed., Academic Press, New York (1962), 96.

(11) SPERA, D.A., "The calculation of elevated-temperature cyclic life considering low-cycle fatigue and creep", ASM Trans., (1969).

(12) WHITE, D.J., "Effect of environment and hold time on the high strain fatigue endurance of ½ per cent molybdenum steel", Proc. Instn. Mech. Eng. 184-1-12 (1969), 223.

(13) COFFIN, L.F., "Fatigue at elevated temperature", The 1972 Symposium on Fatigue at Elevated Temperatures, (1972), 1.

(14) ENDO, K., MIYAO, Y., " Effects of cycle frequency on the corrosion fatigue strength", Trans. JSME, 24-139 (1958).

Table 1 Chemical composition of the materials (%)

Material	C	Si	Mn	P	S	Ni	Cr	Mo	Cu
SUS 32	0.05	0.52	1.72	0.027	0.013	13.60	16.70	2.75	—
SCM 3	0.35	0.25	0.73	0.017	0.005	0.006	0.98	0.17	0.10

Table 2 Mechanical properties of the materials.

Material	Test temp. (°C)	Yielding stress $\sigma_{0.2}$ (kg/mm²)	Tensile strength σ_B (kg/mm²)	Elongation δ(%)	Reduction of area φ(%)	Young's modulus E (kg/mm²)
SUS 32	Room temp.	24.0	55.5	60.5	74.0	2.10×10^4
	550	13.5	41.5	41.5	66.5	1.42
	800	10.1	17.3	75.3	83.0	0.92
SCM 3	Room temp.	90	97	23	62	—
	550	35.5	43.8	25.2	81.4	1.60

Table 3 Experimental Conditions

Material		SUS 32 steel			SCM3 steel
Test temp.		Room temp.	550(°C)	800(°C)	550(°C)
Frequency (Hold time in half cycle)	6cpm (0.3sec)	—	—	—	○ o
	3cpm (5sec)	○	○	○	○
	0.3cpm (95sec)	—	○	○	○ o
	0.03cpm (995sec)	—	—	○	○
Static creep rupture test			—		○

○ in air

o in argon

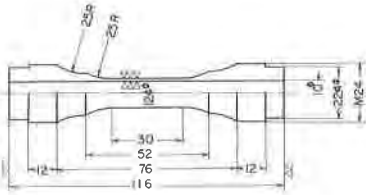

(a) SUS 32 steel

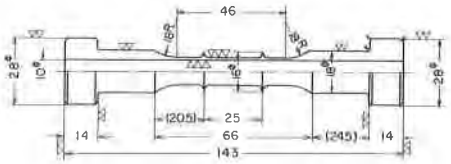

(b) SCM 3 steel

Fig. 1 : Fatigue test specimens.

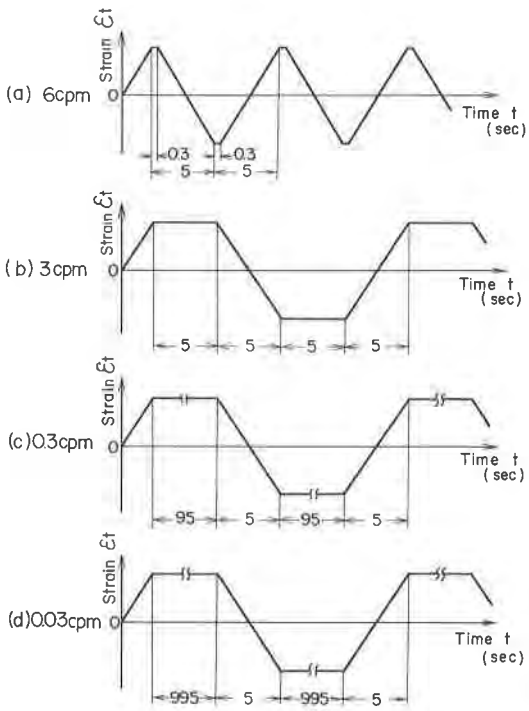

Fig. 2 : Controlled strain waveforms.

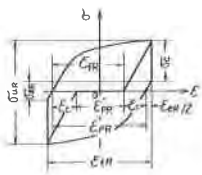

Fig. 3 : Schematic hysteresis loop.

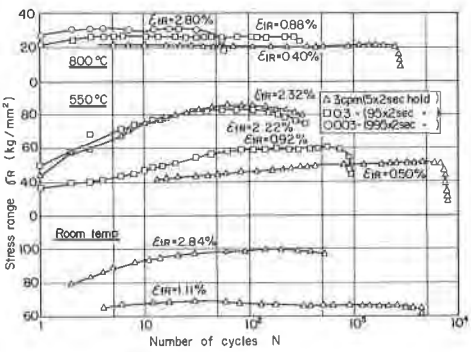

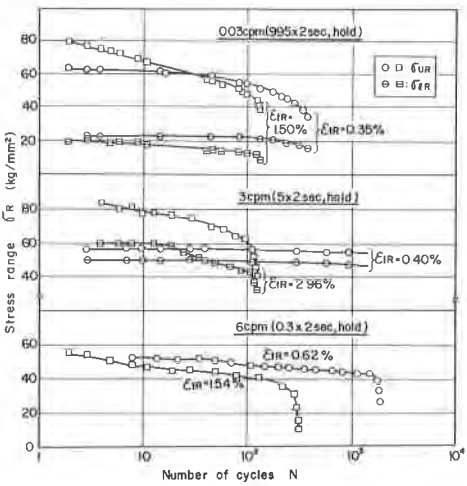

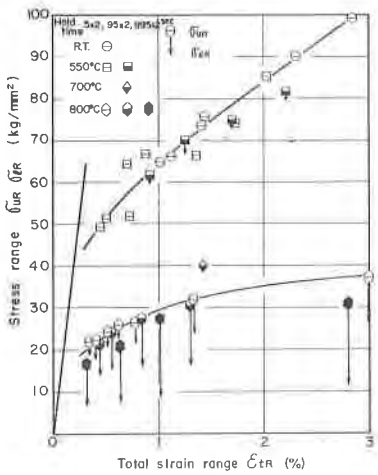

Fig. 6 : Dynamic stress-strain diagrams for SUS32 steel.

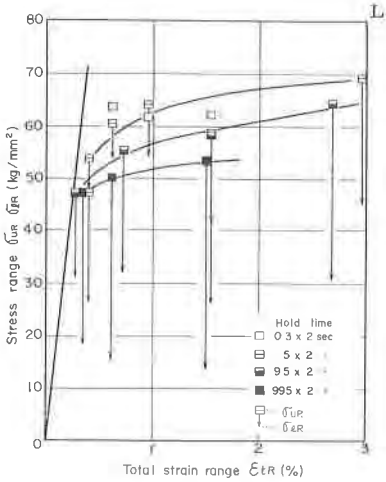

Fig. 7 : Dynamic stress-strain diagrams for SCM 3 steel at 550°C.

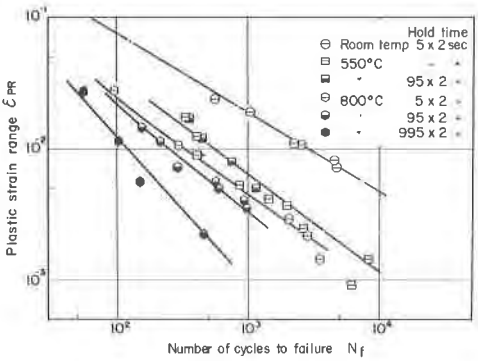

Fig. 8 : Fatigue curves for SUS32 steel. An arrow indicates the number of cycles when temperature fell uncontrollable because of crack initiation at the welding points of thermocouples.

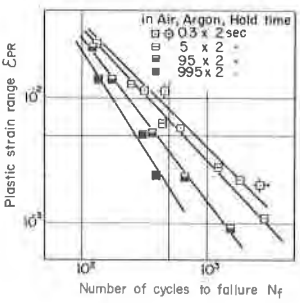

Fig. 9 : Fatigue curves for SCM 3 steel at 550°C. An arrow indicates the number of cycles when temperature fell uncontrollable because of crack initiation at the welding points of thermocouples.

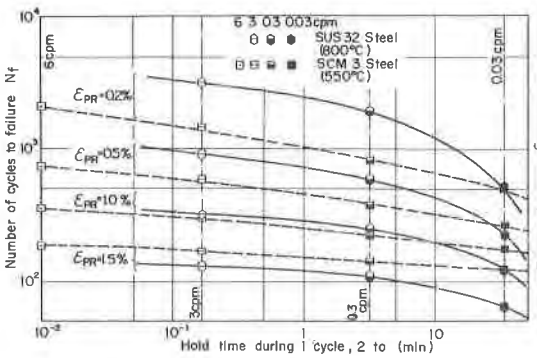

Fig. 10 : Effect of hold time on fatigue life of SUS32 steel and SCM 3 steel

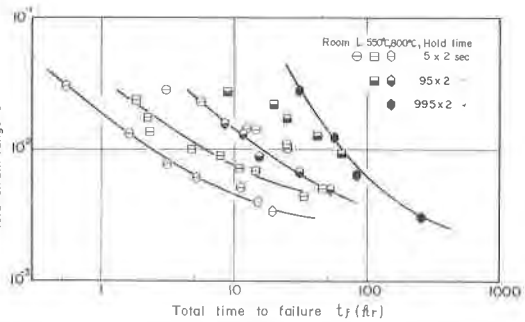

Fig. 11 : Strain range vs. total time to failure for SUS32 steel.

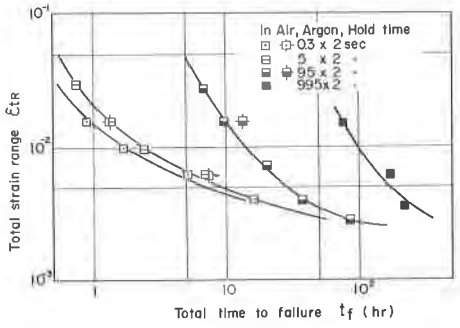

Fig.12 : Strain range vs. total time to failure for SCM 3 steel at 550°C.

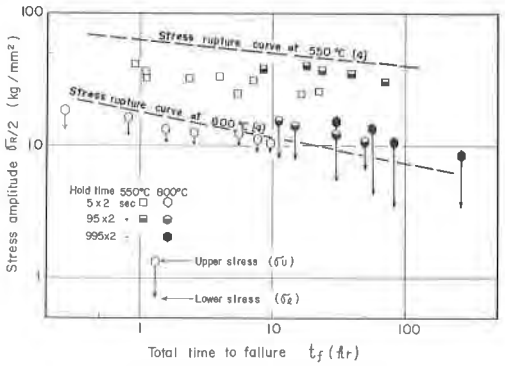

Fig.13 : Applied stress vs. total time to failure for SUS32 steel.

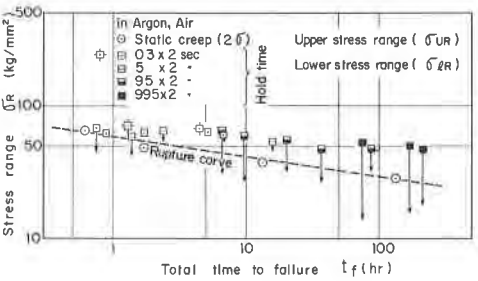

Fig.14 : Applied stress vs. total time to failure for SCM 3 steel at 550°C.

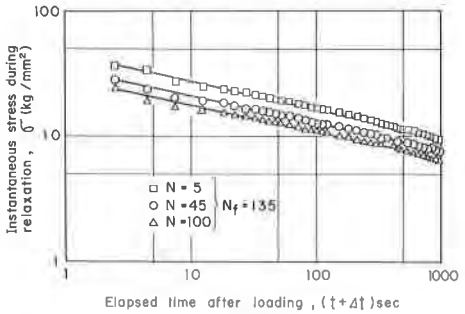

Fig.15 : Typical relaxation curves at the early, middle and latter stages during a fatigue test (in case of SCM 3 steel at 550°C with the hold time of 2 x 995 sec. during a cycle).

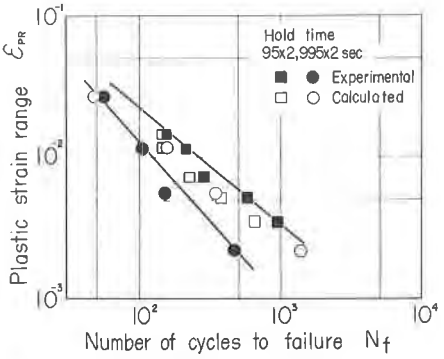

Fig.16 : Comparison of the experimental fatigue life of SUS32 steel at 600°C with the calculated life by Eq. (12) or (13).

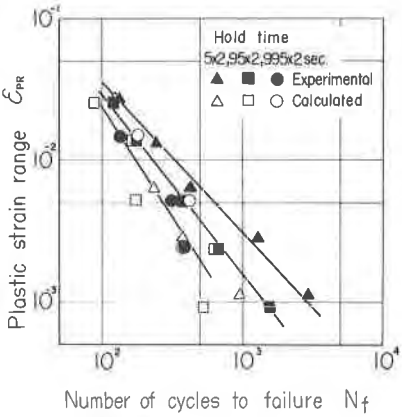

Fig.17 : Comparison of the experimental fatigue life of SCM 3 steel at 550°C with the calculated life by Eq. (12) or (13).

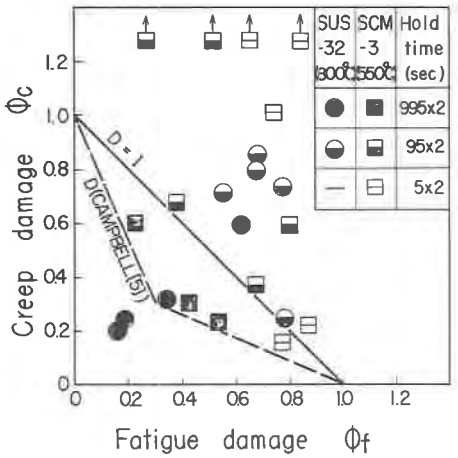

Fig.18 : Correlation between creep damage and fatigue damage by Eq. (7).

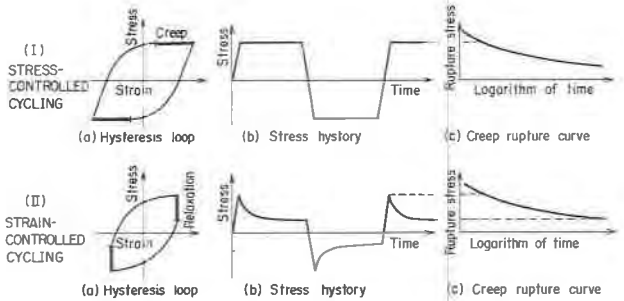

Fig.19 : Comparison of stress-controlled cycling with strain-controlled cycling.

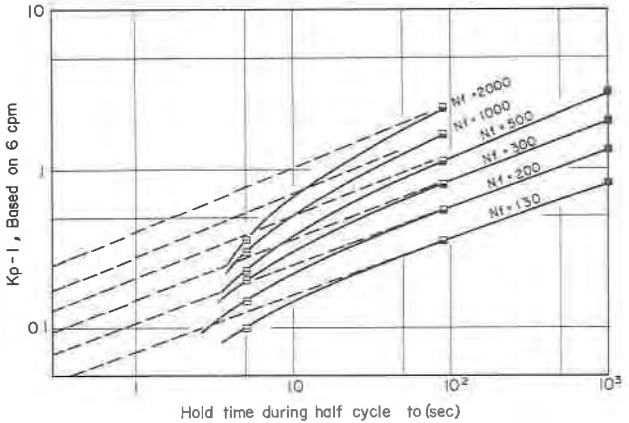

Fig.20 (K_p - 1) vs. t_0 diagram for SCM 3 steel at 550°C.

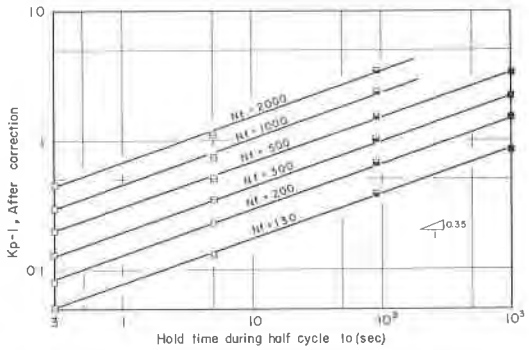

Fig.21 : Corrected (K_p - 1) vs. t_o diagram for SCM 3 steel at 550°C.

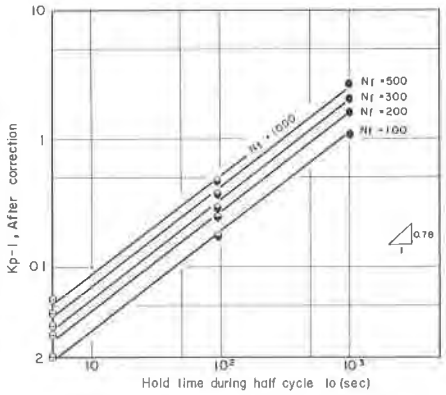

Fig.22 : Corrected (K_p - 1) vs. t_o diagram for SUS32 steel at 800°C

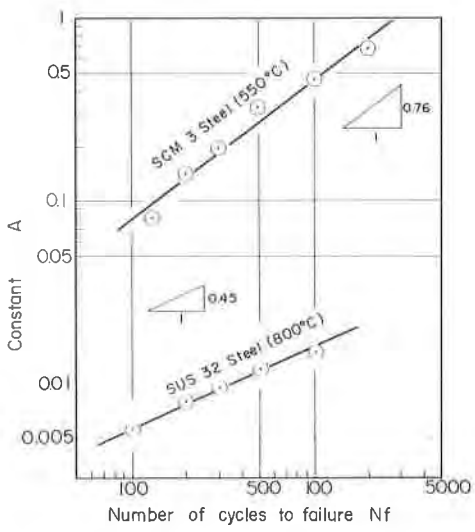

Fig.23 : Correlation between constant A and number of cycles to failure.

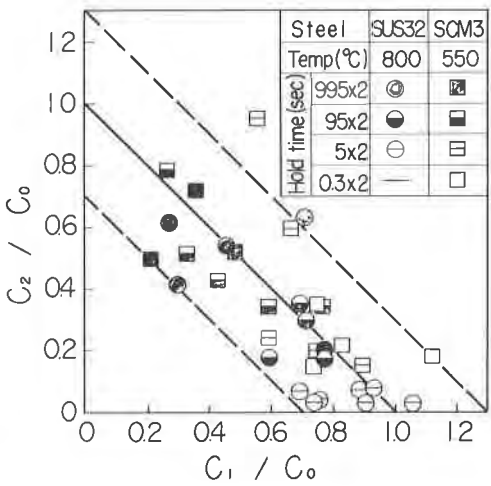

Fig.24 : Correlation between C_1 by Eq. (20) and C_2 by Eq. (21).